

**The influence of tetraphenylethylene moieties on the emissive properties of dipyrrolonaphthyridinediones**

Journal:	<i>Journal of Materials Chemistry C</i>
Manuscript ID	TC-ART-08-2018-003880.R1
Article Type:	Paper
Date Submitted by the Author:	11-Oct-2018
Complete List of Authors:	Sadowski, Bartłomiej; Institute of Organic Chemistry, Polish Academy of Sciences, Su, Shih-Hao; National Taiwan University, Chemistry Lin, Ta-Chun; National Taiwan University, Chemistry Lohrey, Trevor; University of California, Department of Chemistry Deperasińska, Irena; Institute of Physics, ; IF PAN, Chou, Pi-Tai; National Taiwan University, Chemistry Gryko, Daniel; Institute of Organic Chemistry, Polish Academy of Sciences,



Journal Name

ARTICLE

The influence of tetraphenylethylene moieties on the emissive properties of dipyrrolonaphthyridinediones

Received 00th January 20xx,
Accepted 00th January 20xx

Bartłomiej Sadowski,^a Shih-Hao Su,^b Ta-Chun Lin,^b Trevor D. Lohrey,^c Irena Deperasińska,^{*d} Pi-Tai Chou,^{*b} and Daniel T. Gryko^{*a}

DOI: 10.1039/x0xx00000x

www.rsc.org/

Despite being highly emissive in solution, aggregation of dipyrrolonaphthyridinedione (DPND) molecules typically result in the quenching of fluorescence. DPNDs can be efficiently converted into π -extended derivatives containing rotatable aryl rings *via* a direct arylation methodology. The presence of phenyl substituents at positions 3 and 9 of DPND core is sufficient to cause moderate fluorescence in the solid state. When tetraphenylethylene moieties, typical aggregation induced emitters, are coupled through biaryl linkages in these same positions, a 50 nm shift in absorption and almost 120 nm shift in fluorescence compared to the parent DPND is observed. The radiative $S_1 \rightarrow S_0$ transitions have large oscillator strengths regardless if phenyls or tetraphenylethylene groups are coupled to DPND and exhibit strong orange or red emission in solution is observed. Vibrations involving these substituents play an important role in the dissipation of the electronic excitation energy. X-ray crystallographic studies revealed that although the distance between DPND cores is strikingly larger in bis(TPE)₂DPND compared to that in diphenylDPND, their photophysical properties in the solid state are very similar. Computational studies have also shown that, in contrast to our experimental results, neither of these DPNDs should be particularly emissive in the solid state, due to the low oscillator strengths calculated for model dimers derived from their X-ray crystal structures.

Introduction

Research into organic electronic materials is increasingly relevant due to their low cost, light weight and absence of rare earth elements. With the advent of modern technologies such as organic light-emitting diodes,¹ organic field-effect transistors,² sensors³ and advanced fluorescent imaging probes⁴ there is continuous search for novel dyes with improved optoelectronic properties.⁵ Dipyrrolonaphthyridinediones (DPNDs) (Fig. 1a) are a new class of cross-conjugated dyes in which a pyrrole ring constitutes electron-donor moiety and a carbonyl groups act as electron-accepting moiety.⁶ DPNDs possessing alkyl substituents at positions 6 and 12 emit strongly at ~520 nm (Φ_f up to 0.71). From a synthetic point of view, the core can be readily functionalized at positions 3 and 9 using two different synthetic

approaches: 1) selective double bromination followed by a cross-coupling reaction^{6,7} and 2) direct arylation.⁸

X-ray analysis of highly planar DPND molecules reveals they assemble in infinite columnar stacks *via* π - π interactions (Fig 1b).⁶ It has been shown that such an arrangement activates various energy dissipation channels leading to fluorescence quenching in the solid state.⁹ Furthermore, the fluorescence of dyes with such planar structures can also be effectively weakened or even quenched at high concentrations in solution due to the formation of aggregates and is described by the aggregation-caused quenching

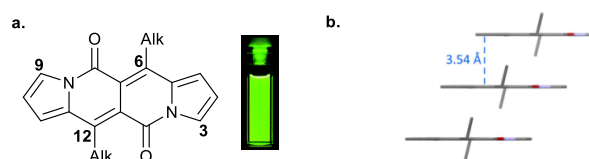


Figure 1. a. Structure, fluorescence and numbering of the key positions of the DPND core. b. Arrangement of DPND molecules in the crystal lattice (view along the chromophore plane).

(ACQ) effect.^{9a} An opposite effect, observed in molecules with less degrees of freedom in the solid state and hence less vibrational deexcitation pathways, was first described by Park and Tang.^{10,11} This aggregation-induced emission (AIE) is mainly responsible for the occurrence of luminescence in the aggregated or in the solid state.^{9b} Many different AIE generators (AIEgens) have been investigated such as

^a Institute of Organic Chemistry, Polish Academy of Sciences, Kasprzaka 44/52, 01-224 Warsaw, Poland, E-mail: dtgryko@icho.edu.pl

^b Department of Chemistry, National Taiwan University, 1 Roosevelt Road Section 4, Taipei 106, Taiwan, E-mail: chop@ntu.edu.tw

^c Department of Chemistry, University of California, Berkeley, 420 Latimer Hall, Berkeley, CA, United States, and Chemical Sciences Division, Lawrence Berkeley National Laboratory, 1 Cyclotron Road, Berkeley, CA, United States, E-mail: tdlohrey@berkeley.edu

^d Institute of Physics, Polish Academy of Sciences, Al. Lotników 32/46, 02-668 Warsaw, Poland, E-mail: deper@ifpan.edu.pl

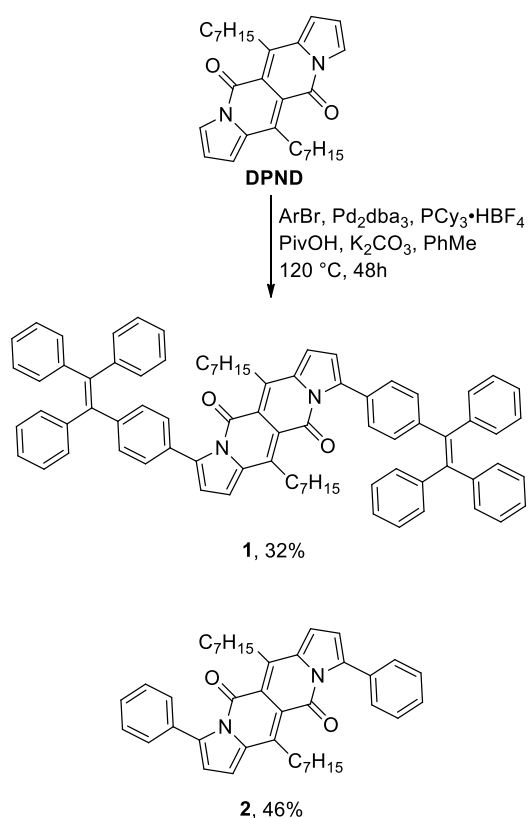
Electronic Supplementary Information (ESI) available: Electrochemical data, computational details, X-ray data and copies of ¹H NMR and ¹³C NMR spectra]. See DOI: 10.1039/x0xx00000x

hexaphenylsiloles,¹² tetraphenylthieno-[3,2-*b*]thiophene *S,S*-dioxides,¹³ diphenylbenzo[*b*]thiophene *S,S*-dioxide,¹⁴ pyrrolo[3,2-*b*]pyrroles¹⁵ and most commonly tetraphenylethylene (TPE).¹⁶ The goal of this investigation is to address the following questions: Is it possible to induce solid state emission in DPND through an appropriate derivatization with TPE moieties?

In this design, the TPE moiety serves several purposes. It is a well-known AIEgen which typically lowers the fluorescence quantum yield in solutions.¹⁷ It will also effectively π -expand the chromophore as it has been proven in our previous studies that aryl linkages in the 3 and 9 positions allow for reasonable electronic coupling with the DPND core.⁸

Results and discussion

Our synthetic strategy towards DPND-based red emitters involves direct arylation of the DPND core (Scheme 1). Using this methodology we successfully obtained derivatives **1** and **2** starting from DPND and either tetraphenylethylene bromide¹⁸ or bromobenzene, respectively.



Scheme 1. Synthesis of DPND derivatives **1** and **2**.

We were able to obtain single crystals of compounds **1** and **2** suitable for X-ray crystallography. Both **1** and **2** crystallize in a triclinic crystal system with the *P*-1 space group, while their unit cells contain one or two molecules of the corresponding dye, respectively (Figure S7). The DPND cores in molecules **1** and **2** generally appear planar – torsion angles between the center of each core and pyrrole ring are

5.7° (molecule **1**) and 4.0° (molecule **2**). In the solid state, molecules of **2** are arranged in infinite columnar stacks in which two different distances between the adjacent DPND core planes can be distinguished: 3.34 Å and 3.43 Å (Figure 2). It seems that multiple C_{aryl}-H...O interactions (2.69 Å, 2.66 Å) play a crucial role in the arrangement in these stacks (Figure S8).

According to X-ray analysis, molecule **1** appears largely planar, with the exception of the phenyl rings of the TPE moiety, which are twisted out of the plane of the two ethylene carbons in the range of 44.1° to 56.5°. In contrast to **2**, the DPND cores of two adjacent molecules of **1** are isolated by a distance of ~7.1 Å from one another (Figure 2), as both faces of these moieties are packed next to non-planar TPE groups on neighboring molecules of **1**. The planar layers within the crystal are also well-separated, on the order of approximately 4.14 Å. These features indicate that this solid phase is free of the π - π interactions that lead to ACQ effects in the parent DPND molecule. Additionally, multiple C_{aryl}-H... π interactions are formed in the crystal lattice of **1** (Figure S8), which should also effectively restrict the phenyl rings of TPE from undergoing intramolecular motions. It should be noted here that for both DPND derivatives **1** and **2**, the dihedral angle between the core and phenyl ring attached to the core at positions 3 and 9 are each ~58°.

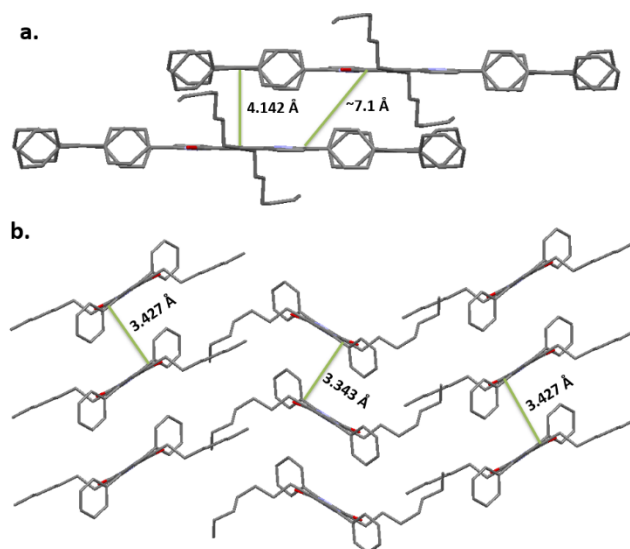


Figure 2. Packing diagram displaying the distances between DPND cores within the crystal lattices of **1** (a) and **2** (b). Hydrogen atoms are omitted for clarity.

Spectroscopic and photophysical properties of derivatives **1** and **2** have been evaluated both in CH₂Cl₂ solution and in the solid state by means of steady-state and time-resolved optical techniques. Absorption and emission spectra are compared in Figures 3 and 4, and the relevant parameters are summarized in Table 1. From Figure 3 and Table 1, it can be seen that the lowest lying absorption maximum of derivative **2** in CH₂Cl₂ is located at 536 nm, while its emission maximum is at 600 nm. The absorption and emission properties of dye **2** in solution are almost identical to the analogous 3,9-diaryIDPNDs published earlier.⁸ The absorption extinction coefficient (ϵ) of $2.4 \times 10^4 \text{ M}^{-1}\text{cm}^{-1}$ and small Stokes shift of $2,000 \text{ cm}^{-1}$ lead us to conclude that the emission originates from a π - π^* transition. The same theoretical basis is also valid to explain the

electronic transition in derivative **1**, although this shows a slightly larger Stokes shift of $2,600\text{ cm}^{-1}$. Compared with derivative **2**, dye **1** bearing two TPE moieties possesses red-shifted absorption and emission maxima. This, together with slightly larger extinction coefficient of $3.1 \times 10^4\text{ cm}^{-1}\text{M}^{-1}$ at the lowest lying absorption maximum, can be attributed to the relatively strong electronic conjugation between DPND core and TPE moiety. The quantum yield of **2** was measured to be 0.71 in dichloromethane, higher than the quantum yield of 0.45 for derivative **1** measured under analogous conditions.

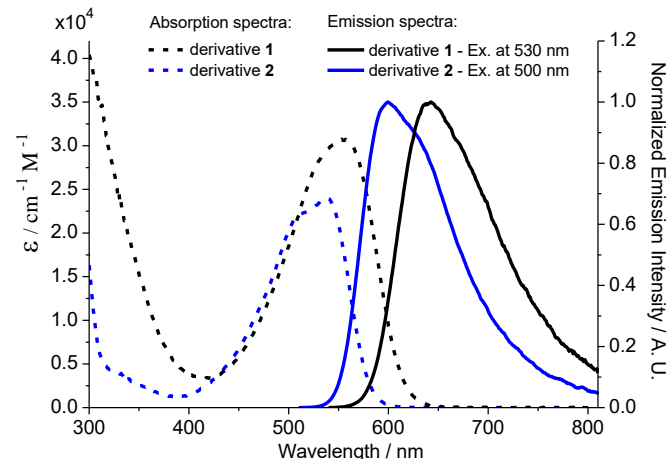


Figure 3. Absorption (dashed line) and normalized emission (solid line) spectra for derivatives **1** and **2** in dichloromethane at room temperature.

Taking the quantum yield (ϕ_f) and the observed lifetime (τ , see Table 1) into account, the radiative rate constant (k_r) and non-radiative rate constant (k_{nr}) of the emission for derivatives **1** and **2** in dichloromethane can be deduced from the relationships $\phi_f = \tau \times k_r$

and $k_{nr} + k_r = \tau^{-1}$. The data listed in Table 1 indicates that the major difference lies in k_{nr} , for which derivative **1** is about three times larger than the value of derivative **2**. Recognizing that the emissions are $> 600\text{ nm}$ for both **1** and **2**, the energy gap law, which specifies an enhanced quenching of fluorescence *via* vibrational overlaps between $S_1 (v' = 0)$ and $S_0 (v = n)$ upon lowering the S_1 - S_0 energy gap,¹⁹ is seemingly observed. Both molecules are large, multi-atomic systems with many vibrational modes capable of acting as acceptors for the dissipated of energy (see below) and are likely to be classified as containing the so-called statistical limit of non-radiative transitions, where the energy gap law operates.^{19,20}

Solid films of **1** and **2** were prepared through spin-coating method. Absorption and emission spectra of derivatives **1** and **2** in these solid films are shown in Figure 4. Compared to their photophysical properties in solution, Figure 4 reveals **1** and **2** undergo a slight red shift in both their absorption and emission spectral features, indicating a non-negligible perturbation by solid-state packing. This can be seen from the reduction in quantum yields for both derivatives **1** and **2** from solution to solid state.

The close proximity of molecules in the crystal lattice results in enhanced intermolecular interactions between them (Figures 2 and S8), which is why we observe the above-mentioned slight red-shift of both the absorption and emission bands as compared to solution state measurements. On the other hand, these smaller Stokes shift values for solid samples can be associated with significant geometrical restrictions of the molecules in the crystal, and thus a smaller distortion of the excited state.

Table 1. Optical and redox properties of DPND, **1** and **2** measured either in dichloromethane solution or in the solid state.

Dye		$\lambda_{\text{abs}}/\text{nm}$	$\epsilon \cdot 10^4 / \text{M}^{-1} \cdot \text{cm}^{-1}$	$\lambda_{\text{em}}/\text{nm}^a$	$\Delta\text{SS}/\text{cm}^{-1}$	ϕ_f	τ/ns	$10^8 \times k_r/\text{s}^{-1}$	$10^8 \times k_{nr}/\text{s}^{-1}$	$E_{\text{HOMO}}/\text{eV}^a$	$E_{\text{LUMO}}/\text{eV}^a$	E_g^{CV}/a
DPND ^b	solution	504	2.9	528	900	0.71	-	-	-	-	-3.30	-
1	solution	553	3.1	644	2600	0.45	2.4	1.9	2.3	-5.30	-3.30	2.00
	solid	574	-	659	2200	0.12	1.3	0.9	6.8	-	-	-
2	solution	536	2.4	599	2000	0.71	4.0	1.8	0.7	-5.36	-3.30	2.06
	solid	562	-	601	1200	0.15	1.1	1.4	7.7	-	-	-

^a Determined based on CV measurements using the equations: $E_{\text{HOMO}} (\text{eV}) = - [E_{\text{ox}}^{\text{onset}} - E^{1/2}(\text{Fc}/\text{Fc}^+) + 4.8]$; $E_{\text{LUMO}} (\text{eV}) = - [E_{\text{red}}^{\text{onset}} - E^{1/2}(\text{Fc}/\text{Fc}^+) + 4.8]$. ^b Taken from Ref. 6.

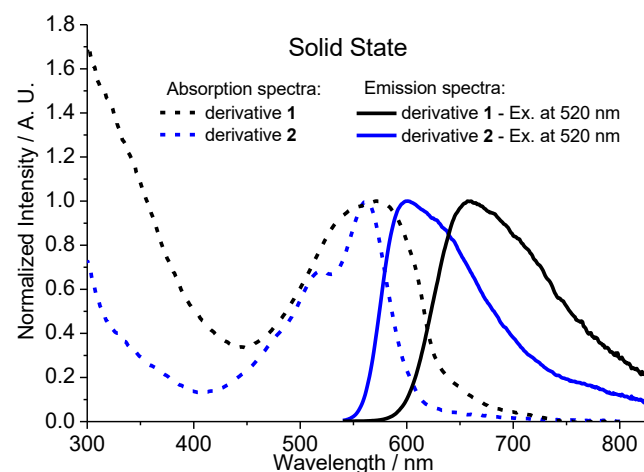


Figure 4. Normalized absorption (dashed line) and emission (solid line) spectra for derivatives **1** and **2** in solid state at room temperature.

According to the literature, there have been a number of reports aiming to transform ACQ materials to AIE materials by adding a TPE moiety.¹⁶ The mechanism behind this transformation is directly linked to the restriction of intramolecular rotations. When these TPE derivatives are in solution, the peripheral phenyl rings may rotate freely, dissipating energy in the excited state. As aggregation takes place, intermolecular stacking prohibits this means of energy dissipation, and thus enhances the luminescence of the material. Conversely, in the case of derivatives **1** and **2**, the π - π stacking quenching mechanism of the DPND core seems to play a greater role than the enhancing effect caused by restricting the rotational freedom of the TPE moiety, which consequently yields a net decrease of the quantum yield in the solid state (cf. in solution).

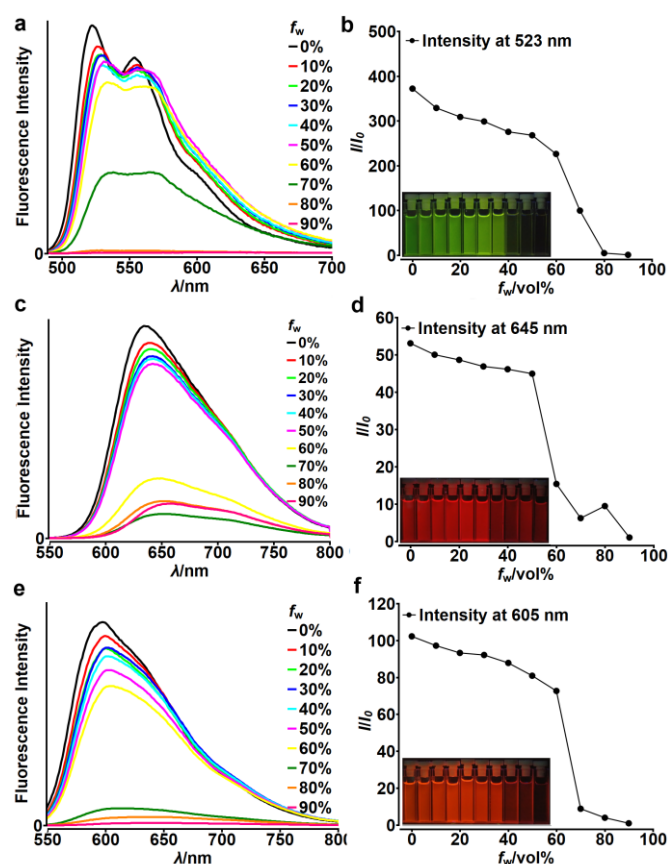


Figure 5. Fluorescence spectra of DPND (a), **1** (c) and **2** (e) in THF-water mixtures of different relative proportions. Plots of maximum intensity vs. % water fraction (f_w) for dyes DPND (b), **1** (d) and **2** (f). Insets: Photographs of DPND (b) and **1** (d) and **2** (e) in THF-water mixtures with different water fractions under UV illumination (0% to 90% water fraction from left to right). Dye concentration: $\sim 10 \mu\text{M}$.

The fluorescence behaviors of DPND, **1** and **2** were investigated in water/THF mixtures (Figure 5). As was suggested in the introductory section, DPND should exhibit a typical ACQ effect. At water fractions equal or higher than 80% the green fluorescence of DPND vanished, which was attributed to this effect. Interestingly, the emission intensity of **1** remained the

same until the f_w value reached 50%, at which point it dropped considerably. The increased hydrophobicity of **1** with respect to DPND is likely responsible for its aggregation at lower water proportions. A modest jump in the emission intensity of **1** upon an increase in the water fraction from 70 to 80% was also observed, possibly related to aggregation effects. Therefore, we concluded that compound **1** shows both ACQ (dominant) and AIE (weak) effects. For dye **2** we observed a similar quenching effect as was observed for DPND; thus it can be also classified solely as an ACQ molecule.

The electrochemical properties of the synthesized compounds were investigated by cyclic voltammetry in dichloromethane. Figure S1 shows the cyclic voltammograms of **1** and **2**, and their electrochemical data are summarized in Table S1. The voltammograms of compounds **1** and **2** show two reduction waves where the first wave is reversible and the latter ones are either quasi-reversible or irreversible. The first reduction wave, assigned previously to electron-transfer to the DPND core,⁸ is characterized by the same potential value for both compounds. Both dyes are characterized by two quasi-reversible, closely lying oxidation waves. Comparing the E_{pa} values for the first oxidation waves (Table S1), dye **1** is slightly more susceptible to oxidation than **2**. On the basis of the first reduction and oxidation waves we also determined the values of E_{HOMO} and E_{LUMO} (Table 1). The E_{LUMO} energy level for both derivatives were calculated to be -3.30 eV , which is a characteristic feature in the majority of the DPND-based dyes.^{6,8} The HOMO level for **2** lies slightly below that for **1**, resulting in a lower electrochemical energy gap (E_g^{CV}) value for the TPE-containing derivative, which is consistent with the optical properties described above.

The detailed results of DFT and TDFT/B3LYP/6-31G(d,p) calculations of the structures and electronic spectra of compounds **1** and **2** are included in the ESI. These are consistent with results for related compounds obtained previously.⁶⁻⁸ The electronic transitions between S_0 and S_1 in molecules **1** and **2** are π - π^* transitions described by the (HOMO, LUMO) configuration, which confirms the previous assumption based on experimental results. The shapes of both orbitals are shown on the diagram of electronic states in Figure 6. It is seen that both the HOMO and LUMO retain the features of the parent DPND molecule with some extension of π -system on the aryl substituents (see also Table S2 and S3 in ESI).

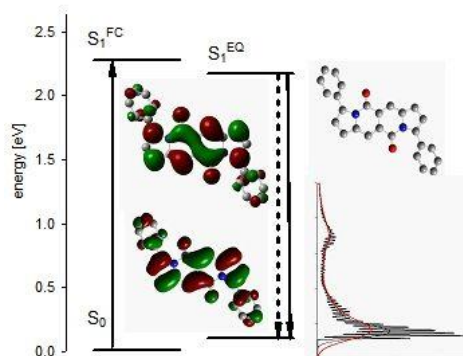


Figure 6. Diagram of electronic states of **2**, shapes of HOMO and LUMO orbitals and simulation of fluorescence of **2** (for details see Figure S4 in ESI).

The calculated transition energies and other parameters (Table S2) are in tolerable agreement²¹ with the experimental data given in Table 1. The substitution of DPND with TPE and C₆H₅ at positions 3 and 9 mainly affects the HOMO energy level, causing a red shift in both absorption and fluorescence and increasing the oscillator strength of the S₀ → S₁ transition. The characteristic features of the structure optimized in the excited state S₁ is a decrease in the dihedral angle between the aryl rings of the substituents and the DPND core from ~45° to ~35°. This is accompanied by a slight increase in the oscillator strength of the S₁ → S₀ transition.

Our calculations involved the simulation of the fluorescence spectrum as an electron-vibrational spectrum (Insert Figure 6, Figure S4) based on calculations of Franck-Condon factors (Table S4).²² These calculations show that in the S₁ → S₀ transition for molecule **2**, low frequency vibrations are an active pathway for decay. The movement of the aryl substituents play a significant role in these vibrations. As a consequence, the electronic spectrum is blurred, resulting in a wide, unstructured band.

High values of Franck-Condon factors for vibrations involving substituents indicate their important role in the dissipation of energy from electronic excitation. The TPE and C₆H₅ substituents attached to DPND in the 3 and 9 positions have restricted internal rotation leading to two potential minima on the potential energy surface (Figure S2). These two minima correspond to the previously identified C₁ and C₂ isomers⁸ (also optimized in this work – see Table S2). The height of the barriers between these is controlled by steric factors. The small barrier is connected to the path with the substituent plane perpendicularly oriented to the DPND plane and larger barrier corresponds to the parallel arrangement of both planes (Figure S2).

The mutual orientation of the DPND core and the substituents controls the magnitude of the oscillator strength of the S₀ → S₁ transition. This is shown in Figure S3. Their coplanarity, favoring the π-system extension on the whole molecule, leads to the high values of the oscillator strength. On the other hand, the lowest excited state S₁ becomes the CT state (charge-transfer from the substituent to the DPND center - see Figure S3) with the oscillator strength being virtually zero for perpendicular TPE and DPND planes (Figure S3).

The four types of dimers extracted from the crystallographic structure of DPND⁶ are systems with low or zero oscillator strengths for the transition between the states S₀ and S₁, which makes the DPND an ACQ-type molecule. In the case of two dimers, the transition between S₀ and S₁ is an intermolecular CT transition, *i.e.* HOMO (monomer 2) → LUMO (monomer 1), in which the CT state has a high dipole moment.

Seeking an explanation of the ACQ effect observed for the fluorescence spectra in THF/water mixtures, we carried out calculations of electronic states of DPND dimers. These dimers are formed by selecting monomer pairs from the DPND crystal.⁶ The results shown in Table S5 indicate that all four dimers are characterized by a low or zero oscillator strength for the

transition between the S₀ and S₁ states. Such a result justifies DPND and its derivatives to be ACQ in nature.

Moreover, the electronic states of two of the dimers are located on only one of the components. In particular, the S₁ state of such a dimer is an intermolecular charge-transfer state with the charge transfer from one monomer to the other. This state is characterized by a large dipole moment and is stabilized with the increasing polarity of the surroundings. Accordingly, the effect observed in THF-water mixtures is undoubtedly related to the increasing polarity of the solvent.²³ Therefore, this quenching mechanism can be proposed as the process leading to the deactivation of the excited states of such solution based dimers.

The calculated energies and oscillator strengths of electronic transitions in selected dimers of **1** and **2** (shown in Tables S10 and S11) are similar to results obtained for DPND (*i.e.* the S₀ → S₁ transition in most of cases is characterized by zero or low oscillator strength). However, dimers in which the DPND cores are oriented in an approximately linear fashion (so-called head-to-tail) diverge from this regularity. The coordinates of the atoms in the B dimer of DPND **2** are given in Table S12. This dimer is a J type aggregate, according to the nomenclature prescribed by the exciton model in molecular spectroscopy.²⁴ The second type of aggregates described by this model are H-aggregates, with sandwich (face-to-face) ordering of monomers (dimers A and C in Table S11). In the model dimers, pairs of degenerate monomeric electronic states are split due to the coupling between the moments of their dipole transitions. The mutual orientation of the transition moments in J-aggregates leads to an amplification of transition intensity in the dimer compared to the monomer, while in H-aggregates this mutual orientation leads to the reverse, a decrease in intensity. It is obvious that real systems represent intermediate cases between H and J-aggregates and, moreover, that this analysis of the effect of dimer interactions, truncated from the crystalline environment, are only an approximation of reality.

In all, the calculations carried out for selected dimers of DPND, **1**, and **2** confirm the experimental results, implying there is no or weak AIE effect in these systems. The results also indicate, however, that such an effect could be observed by manipulating the geometric structure of these compounds. Lastly, the calculations show that the effects of AIE can be interpreted as part of the exciton model in molecular spectroscopy.

Conclusions

In this study we have shown that the presence of a tetraphenylethylene moiety does not always cause a decrease in the emission intensity of solutions of organic dyes. In spite of the fact that there is strong electronic communication between TPE moieties and the dipyrrolonaphthyridinedione core, the dye displays red fluorescence both in solution and in the solid state. The effect on the fluorescence in the crystalline state is not drastically different when compared to attachment of simple phenyl groups. The gathered evidence suggests that the rationale behind this phenomenon is the fact that the phenyl

rings directly attached DPND core are significantly conjugated with it.²⁶ Consequently tetraphenylethylene moiety does not play its usual role as quencher of fluorescence in the solution.

Experimental

Materials and methods

All reagents and solvents were purchased from commercial sources and were used as received unless otherwise noted. Reagent grade solvents (CH₂Cl₂, cyclohexane) were distilled prior to use. Toluene was dried by distillation over sodium and stored under argon. Transformations with moisture- and oxygen-sensitive compounds were performed under a stream of argon. The reaction progress was monitored by means of thin-layer chromatography (TLC), which was performed on aluminum foil plates, covered with silica gel 60 F254 or aluminum oxide 60 F254 (neutral). Product purifications were done by means of column chromatography with Kieselgel 60. The identity and purity of prepared compounds were proved by ¹H NMR and ¹³C NMR spectrometry as well as by mass spectrometry (via EI-MS or ESI-MS). HRMS (ESI-TOF) and HRMS (EI): double-focusing magnetic sector instruments with EBE geometry were utilized. NMR spectra were measured on 500 or 600 MHz instruments. Chemical shifts were determined with tetramethylsilane (TMS) as the internal reference. All melting points for crystalline products were measured with an automated melting point apparatus and are given without correction. DPND⁶ and tetraphenylethylene bromide¹⁸ were synthesized as described earlier.

Optical measurements

A Hitachi (U-3310) spectrophotometer and an Edinburgh (FS920) fluorimeter were used to acquire steady-state absorption and emission spectra, respectively. Photoluminescence (PL) spectra of thin films were characterized by a spectrofluorimeter (FluoroMax-P, Horiba Jobin Yvon Inc.). Photoluminescence quantum yields (ϕ_{PL}) of thin films or dilute solutions were determined using this spectrofluorimeter equipped with a calibrated integrating sphere. Nanosecond time-resolved studies were performed with an Edinburgh FL 900 time-correlated single photon-counting (TCSPC) system.

X-Ray Crystallography

The solid-state structure of **1** was determined the Advanced Light Source (ALS) beam line 12.2.1, located at Lawrence Berkeley National Laboratory. A red, plate-shaped crystal of **1** selected from the bulk material was mounted onto a polymer loop and cooled in a 100 K stream of dry nitrogen. Diffraction data was collected using a silicon-monochromated beam of 17 keV (0.7288 Å) synchrotron radiation, and a Bruker D8 diffractometer equipped with a Bruker Photon II CPAD detector. The structure was corrected for absorption using a multi-scan method (SADABS), solved using SHELXT, and refined against F^2 using SHELXL-2014. Publication materials were made using WinGX. Single crystal of compound **2** was achieved from slow evaporation of hexanes/ethyl acetate solution at room

temperature. Single-crystal X-ray-diffraction data were obtained from a Bruker D8 VENTURE Single-crystal XRD equipped with Oxford Cryostream 800+ at the temperature of 200 K. Structures of the crystals were solved by direct methods using the SHELXS-97 software. None-hydrogen atoms were refined anisotropically by full-matrix least-squares calculations on F^2 using SHELXL-97, while the hydrogen atoms were introduced at calculated position and refined in the riding mode. Structures of **1** and **2** has been submitted to the Cambridge Crystallographic Data Centre, with the deposition number CCDC 1870308 and CCDC 1871705, respectively. Drawings were produced using Mercury.

Computational studies

Calculations based upon the optimized structure of the molecules in both the ground state (S_0) and the lowest electronically excited state (S_1) were made using the DFT and TDDFT / B3LYP / 6-31G(d,p) methods. The calculations used Gaussian 09.²⁵

Synthetic procedures

General procedure for direct arylation of DPND

In a 25 mL Schlenk flask containing a magnetic stirring bar were placed: DPND (0.1 mmol, 43.3 mg, 1.0 eq), tris(dibenzylideneacetone)dipalladium(0) (9.4 mg, 0.01 mmol, 10 mol%), PCy₃-HBF₄ (7.4 mg, 0.02 mmol, 20 mol%), pivalic acid (6.2 mg, 0.06 mmol, 60 mol%), K₂CO₃ (55.2 mg, 0.4 mmol, 4.0 eq) and the bromoarene (0.27 mmol, 2.7 eq). The vessel was evacuated and backfilled with argon (3 times). If the haloarene (0.27 mmol, 2.7 eq) was a liquid it was added next using a syringe followed by anhydrous, degassed toluene (2 mL). The vessel was tightly closed and again carefully evacuated and backfilled with argon (3 times). The content of the flask was stirred at 120 °C for 48 h. After that time the flask was cooled down to RT and extracted three times with dichloromethane (3 x 20 mL), then dried over magnesium sulphate. All solvents were evaporated off and the residue was purified by column chromatography (SiO₂, cyclohexane : dichloromethane = 2:1). All further manipulations are described below.

6,12-Diheptyl-3,9-bis(4-(1,2,2-triphenylvinyl)phenyl)-5H,11H-dipyrrolo[1,2-b:1',2'-g][2,6]naphthyridine-5,11-dione (**1**)

Prepared using tetraphenylethylene bromide (111.2 mg, 0.27 mmol). After column chromatography all solvents were evaporated off, then the residue was boiled in cyclohexane and cooled overnight in the fridge. The crystals were filtered off, washed with *n*-pentane and dried under high vacuum to give 35.0 mg (32% yield) of product. R_f = 0.31 (SiO₂, cyclohexane/dichloromethane, 2:1). Mp. 247-248 °C (dec.); ¹H NMR (600 MHz, CD₂Cl₂, 25 °C): δ = 7.23 (d, J = 8.4 Hz, 4H), 7.19-7.11 (m, 26H), 7.07-7.03 (m, 8H), 6.87 (d, J = 3.6 Hz, 2H), 6.50 (d, J = 4.2 Hz, 2H), 3.17-3.15 (m, 4H), 1.66-1.61 (m, 4H), 1.49-1.43 (m, 4H), 1.38-1.28 (m, 12H), 0.90 ppm (t, 6H, J = 6.6 Hz); ¹³C NMR (151 MHz, CD₂Cl₂) δ 159.6, 143.8, 143.7, 143.7, 143.1, 143.0, 141.4, 140.6, 139.7, 135.5, 131.3, 131.1, 131.1, 130.3, 127.8, 127.7, 127.7, 127.6, 126.5, 126.4, 126.3, 118.2, 115.7, 115.4, 31.9, 30.6, 30.3, 30.2, 29.2, 22.7, 13.9; HRMS (ESI): m/z

calcd for $C_{80}H_{72}N_2O_2Na$ 1115.5491 [M+Na⁺], found 1115.5497; Anal. Calcd. for $C_{80}H_{72}N_2O_2$: C, 87.87; H, 6.64; N, 2.56; Found: C, 87.75; H, 6.78; N, 2.37.

6,12-Diheptyl-3,9-diphenyl-5H,11H-dipyrrolo[1,2-b:1',2'-g][2,6]naphthyridine-5,11-dione (2)

Prepared using bromobenzene (42.4 mg, 0.27 mmol, 28.4 μ L). After column chromatography all solvents were evaporated off, then the residue was reprecipitated from dichloromethane/methanol mixture, filtered off and dried under high vacuum to give 27.0 mg (46% yield) of product. R_f = 0.43 (SiO₂, cyclohexane/dichloromethane, 2:1). Mp. 190-191 °C; ¹H NMR (500 MHz, CD₂Cl₂, 25 °C): δ = 7.50 (d, J = 7.0 Hz, 4H), 7.43-7.37 (m, 6H), 6.92 (d, J = 4.0 Hz, 2H), 6.54 (d, J = 3.5 Hz, 2H), 3.23-3.20 (m, 4H), 1.70-1.64 (m, 4H), 1.51-1.45 (m, 4H), 1.39-1.31 (m, 12H), 0.90 ppm (t, 6H, J = 7.0 Hz); ¹³C NMR (125 MHz, CD₂Cl₂, 25 °C): δ = 159.7, 143.3, 139.8, 135.3, 133.3, 128.7, 127.7, 127.5, 118.2, 115.7, 115.5, 31.8, 30.5, 30.3, 30.2, 29.2, 22.7, 13.8 ppm; HRMS (EI): m/z calcd for $C_{40}H_{44}N_2O_2$ 584.3403 [M⁺], found 584.3395.

Acknowledgements

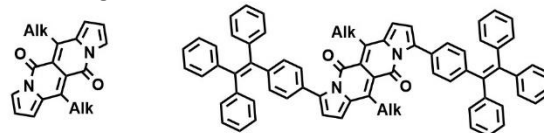
The work was financially supported by the Polish National Science Centre (Grant No. PRELUDIUM 2016/23/N/ST5/00054). The authors would like to thank the Foundation for Polish Science (Grant TEAM/2016-3/22) and Global Research Laboratory Program (2014K1A1A2064569) through the National Research Foundation (NRF) funded by Ministry of Science, ICT & Future Planning (Korea). Theoretical calculations were done at the interdisciplinary Center of Mathematical and Computer Modeling (ICM) of the Warsaw University under the computational grant No. G-32-10. We thank Dr. Simon J. Teat for training and guidance throughout our diffraction studies at ALS station 12.2.1. The Advanced Light Source is supported by the Director, Office of Science, Office of Basic Energy Sciences, of the U.S. Department of Energy under Contract No. DE-AC02-05CH11231.

Notes and references

- (a) L.-S. Cui, Y.-L. Deng, D. P.-K. Tsang, Z.-Q. Jiang, Q. Zhang, L.-S. Liao and C. Adachi, *Adv. Mater.*, 2016, **28**, 7620-7625. (b) D. Chen, S.-J. Su and Y. Cao, *J. Mater. Chem. C*, 2014, **2**, 9565. (c) X. Yang, X. Xu and G. Zhou, *J. Mater. Chem. C*, 2015, **3**, 913. (d) R. Komatsu, H. Sasabe, Y. Seino, K. Nakao and J. Kido, *J. Mater. Chem. C*, 2016, **4**, 2274 (e) Y. Cai, C. Shi, H. Zhang, B. Chen, K. Samedov, M. Chen, Z. Wang, Z. Zhao, X. Gu, D. Ma, A. Qin and B. Z. Tang, *J. Mater. Chem. C*, 2018, **6**, 6534. (f) K. Miyamoto, T. Sawada, H. Jintoku, M. Takafuji, T. Sagawa and H. Ihara, *Tetrahedron Lett.*, 2010, **51**, 4666.
- (a) M. Stolte, S.-L. Suraru, P. Diemer, T. He, C. Burschka, U. Zschieschang, H. Klauk and F. Würthner, *Adv. Funct. Mater.*, 2016, **26**, 7415-7422. (b) T. Uemura, C. Rolin, T.-H. Ke, P. Fesenko, J. Genoe, P. Heremans and J. Takeya, *Adv. Mater.*, 2016, **28**, 151-155. (c) X. Zhang, Y. Zhen, X. Fu, J. Liu, X. Lu, P. He, H. Dong, H. Zhang, G. Zhao, L. Jiang and W. Hu, *J. Mater. Chem. C*, 2014, **2**, 8222. (d) F. Paulus, B. D. Lindner, H. Reiß, F. Rominger, A. Leineweber, Y. Vaynzof, H. Sirringhaus and U. H. F. Bunz, *J. Mater. Chem. C*, 2015, **3**, 1604.
- (a) J. Chan, S. C. Dodani and C. J. Chang, *Nature Chem.*, 2012, **4**, 973-983. (b) N. M. Bojanowski, F. Hainer, M. Bender, K. Seehafer and U. H. F. Bunz, *Chem. Eur. J.*, 2018, **24**, 4255-4258. (c) R. T. K. Kwok, C. W. T. Leung, J. W. Y. Lam and B. Z. Tang, *Chem. Soc. Rev.*, 2015, **44**, 4228. (d) Y. Kim, M. Choi, S. V. Mulay, M. Jang, J. Y. Kim, W. Lee, S. Jon and D. G. Churchill, *Chem. Eur. J.*, 2018, **24**, 5623. (e) T. Yudhistira, S. V. Mulay, K. J. Lee, Y. Kim, H.-S. Park and D. G. Churchill, *Chem. Asian J.*, 2017, **12**, 1927. (f) J. Han, C. Ma, B. Wang, M. Bender, M. Bojanowski, M. Hergert, K. Seehafer, A. Herrmann and U. H. F. Bunz, *Chem*, 2017, **2**, 817-824.
- (a) J. B. Grimm, A. J. Sung, W. R. Legant, P. Hulamm, S. M. Matlosz, E. Betzig and L. D. Lavis, *ACS Chem. Biol.*, 2013, **8**, 1303. (b) A. N. Butkevich, G. Yu. Mitronova, S. C. Sidenstein, J. L. Klocke, D. Kamin, D. N. H. Meineke, E. D'Este, P.-T. Kraemer, J. G. Danzl, V. N. Belov and S. W. Hell, *Angew. Chem. Int. Ed.*, 2016, **55**, 3290-3294. (c) A. L. Antaris, H. Chen, K. Cheng, Y. Sun, G. Hong, C. Qu, S. Diao, Z. Deng, X. Hu, B. Zhang, X. Zhang, O. K. Yaghi, Z. R. Alamparambil, X. Hong, Z. Cheng and H. Dai, *Nature Mat.*, 2016, **15**, 235-243. (d) W. Xu, Z. Zeng, J.-H. Jiang, Y.-T. Chang and L. Yuan, *Angew. Chem. Int. Ed.*, 2016, **55**, 13658-13699. (e) A. T. Wrobel, T. C. Johnstone, A. Deliz Liang, S. J. Lippard and P. Rivera-Fuentes, *J. Am. Chem. Soc.*, 2014, **136**, 4697-4705. (f) J. Yin, Y. Hu and J. Yoon, *Chem. Soc. Rev.*, 2015, **44**, 4619.
- (a) C. Wang, A. Fukazawa, M. Taki, Y. Sato, T. Higashiyama and S. Yamaguchi, *Angew. Chem., Int. Ed.*, 2015, **54**, 15213. (b) L. D. Lavis, *Biochemistry*, 2017, **56**, 5165. (c) A. Gandioso, R. Bresolí-Obach, A. Nin-Hill, M. Bosch, M. Palau, A. Galindo, S. Contreras, A. Rovira, C. Rovira, S. Nonell and V. Marchán, *J. Org. Chem.*, 2018, **83**, 1185. (d) M. Y. Fu, Y. Xiao, X. H. Qian, D. F. Zhao and Y. F. Xu, *Chem. Commun.*, 2008, **15**, 1780-1782. (e) Y. Koide, Y. Urano, K. Hanaoka, T. Terai, T. Nagano, *J. Am. Chem. Soc.*, 2011, **133**, 5680. (f) Y. Koide, K. Urano, T. Hanaoka, Terai and T. Nagano, *ACS Chem. Biol.*, 2011, **6**, 600. (g) K. Namba, A. Mera, A. Osawa, E. Sakuda, N. Kitamura and K. Tanino, *Org. Lett.*, 2012, **14**, 5554. (h) A. Janiga, E. Glodkowska-Mrowka, T. Stoklosa and D. T. Gryko, *Asian J. Org. Chem.*, 2013, **2**, 411. (i) M. Grzybowski, M. Taki and S. Yamaguchi, *Chem. Eur. J.*, 2017, **23**, 13028-13032.
- M. Grzybowski, I. Deperasińska, M. Chotkowski, M. Banasiewicz, A. Makarewicz, B. Kozankiewicz and D. T. Gryko, *Chem. Commun.*, 2016, **52**, 5108.
- B. Sadowski, H. Kita, M. Grzybowski, K. Kamada and D. T. Gryko, *J. Org. Chem.*, 2017, **82**, 7254.
- B. Sadowski, M. F. Rode and D. T. Gryko, *Chem. Eur. J.*, 2018, **24**, 855.
- (a) B. Birks, *Photophysics of Aromatic Molecules*, Wiley, London, 1970. (b) Y. Hong, J. W. Y. Lam and B. Z. Tang, *Chem. Soc. Rev.*, 2011, **40**, 5361.
- (a) J. Luo, Z. Xie, J. W. Y. Lam, L. Cheng, H. Chen, C. Qiu, H.S. Kwok, X. Zhan, Y. Liu, D. Zhu and B. Z. Tang, *Chem. Commun.*, 2001, 1740-1741. (b) B.-K. An, S.-K. Kwon, S.-D. Jung and S. Y. Park, *J. Am. Chem. Soc.*, 2002, **124**, 14410. (c) B. Z. Tang, X. Zhan, G. Yu, P. P. Sze Lee, Y. Liu and D. Zhu, *J. Mater. Chem.*, 2001, **11**, 2974. (d) B.-K. An, J. Gierschner and S. Y. Park, *Acc. Chem. Res.*, 2012, **45**, 544.
- N. L. C. Leung, N. Xie, W. Yuan, Y. Liu, Q. Wu, Q. Peng, Q. Miao, J. W. Y. Lam and B. Z. Tang, *Chem. Eur. J.*, 2014, **20**, 15349.
- (a) Y. Hong, J. W. Y. Lam, B.Z. Tang, *Chem. Commun.*, 2009, 4332-4353. (b) G. Lin, L. Chen, H. Peng, S. Chen, Z. Zhuang, Y. Li, B. Wang, Z. Zhao and B. Z. Tang, *J. Mater. Chem. C*, 2017, **5**, 4867.
- B. Chen, H. Zhang, W. Luo, H. Nie, R. Hu, A. Qin, Z. Zhao and B. Z. Tang, *J. Mater. Chem. C*, 2017, **5**, 960.
- J. Guo, S. Hu, W. Luo, R. Hu, A. Qin, Z. Zhao and B. Z. Tang, *Chem. Commun.*, 2017, **53**, 1463-1466.

- 15 (a) K. Li, Y. Liu, Y. Li, Q. Feng, H. Hou and B. Z. Tang, *Chem. Sci.*, 2017, **8**, 7258. (b) Y. Ji, Z. Peng, B. Tong, J. Shi, J. Zhi and Y. Dong, *Dyes Pigm.*, 2017, **139**, 664. (c) B. Sadowski, K. Hassanein, B. Ventura and D. T. Gryko, *Org. Lett.*, 2018, **20**, 3183.
- 16 (a) Q. Zhao, S. Zhang, Y. Liu, J. Mei, S. Chen, P. Lu, A. Qin, Y. Ma, J. Zhi Sun and B. Z. Tang, *J. Mater. Chem.*, 2012, **22**, 7387. (b) N.-H. Xie, C. Li, J.-X. Liu, W.-L. Gong, B. Z. Tang, G. Li and M.-Q. Zhu, *Chem. Commun.*, 2016, **52**, 5808-5811. (c) Q. Zhao, X. A Zhang, Q. Wei, J. Wang, X. Y. Shen, A. Qin, J. Zhi Sun and B. Z. Tang, *Chem. Commun.*, 2012, **48**, 11671-11673. (d) A. Qin, J. W. Y. Lam and B. Z. Tang, *Prog. Polym. Sci.*, 2012, **37**, 182.
- 17 Aggregation-Induced Emission: Fundamentals and Applications, Volumes 1 and 2, Eds.: A. Qin and B. Z. Tang, 2014, Wiley.
- 18 X. Zhang, Z. Chi, H. Li, B. Xu, X. Li, S. Liu, Y. Zhang and J. Xu, *J. Mater. Chem.*, 2011, **21**, 1788.
- 19 R. Englman and J. Jortner, *Mol. Phys.*, 1970, **18**, 145.
- 20 (a) A. Tramer, Ch. Jungen and F. Lahmani, *Energy Dissipation in Molecular Systems*, Springer-Verlag Berlin Heidelberg 2005. (b) J. Lakowicz, *Principles of Fluorescence Spectroscopy*, New York: Kluwer Academic/Plenum, 1999.
- 21 (a) M. Parac and S. Grimme, *Chem. Phys.* 2003, **292**, 11. (b) J. Tao, S. Tretiak, J.-X. Zhu, *Phys. Rev. B* 2009, **80**, 235110. (c) A. K. Pati, S. J. Gharpure and A. K. Mishra, *Phys. Chem. Chem. Phys.*, 2014, **16**, 14015. (d) J. Kim, K. Hong, S.-Y. Hwang, S. Ryu, S. Choi and W. Y. Kim, *Phys. Chem Chem. Phys.*, 2017, **19**, 10177.
- 22 (a) V. Barone, J. Bloino, M. Biczysko and F. Santoro, *J. Chem. Theory Comput.*, 2009, **5**, 540. (b) J. Bloino, M. Biczysko, F. Santoro and V. Barone, *J. Chem. Theory Comput.*, 2010, **6**, 1256.
- 23 Dielectric Constant and Refractive Index from 20 to 35° and Density at 25° C for the System Tetrahydrofuran/Water: F. E. Critchfield, J. A. Gibson Jr. and J. L. Hall, *J. Am. Chem. Soc.*, 1953, **75**, 6044.
- 24 (a) M. Kasha, H. R. Rawls and M. A. El-Bayoumi, *Pure Appl. Chem.*, 1965, **11**, 371. (b) A. Eisfeld and J.S. Briggs, *Chemical Physics*, 2006, **324**, 376. (c) T. Eder, T. Stangl, M. Gmelch, K. Remmerssen, D. Laux, S. Höger, J. M. Lupton and J. Vogelsang, *Nat. Commun.*, 2017, **8**, 1641. (d) M. Bayda, F. Dumoulin, G. L. Hug, J. Koput, R. Gorniak and A. Wojcik, *Dalton Trans.*, 2017, **46**, 1914. (e) A. Celestino and A. Eisfeld, *J. Phys. Chem. A*, 2017, **121**, 5948.
- 25 M. J. Frisch, G. W. Trucks, H. B. Schlegel, G. E. Scuseria, M. A. Robb, J. R. Cheeseman, G. Scalmani, V. Barone, B. Mennucci, G. A. Petersson, H. Nakatsuji, M. Caricato, X. Li, H. P. Hratchian, A. F. Izmaylov, J. Bloino, G. Zheng, J. L. Sonnenberg, M. Hada, M. Ehara, K. Toyota, R. Fukuda, J. Hasegawa, M. Ishida, T. Nakajima, Y. Honda, O. Kitao, H. Nakai, T. Vreven, J. A. Montgomery, Jr., J. E. Peralta, F. Ogliaro, M. Bearpark, J. J. Heyd, E. Brothers, K. N. Kudin, V. N. Staroverov, R. Kobayashi, J. Normand, K. Raghavachari, A. Rendell, J. C. Burant, S. S. Iyengar, J. Tomasi, M. Cossi, N. Rega, J. M. Millam, M. Klene, J. E. Knox, J. B. Cross, V. Bakken, C. Adamo, J. Jaramillo, R. Gomperts, R. E. Stratmann, O. Yazyev, A. J. Austin, R. Cammi, C. Pomelli, J. W. Ochterski, R. L. Martin, K. Morokuma, V. G. Zakrzewski, G. A. Voth, P. Salvador, J. J. Dannenberg, S. Dapprich, A. D. Daniels, O. Farkas, J. B. Foresman, J. V. Ortiz, J. Cioslowski and D. J. Fox, *Gaussian 09 (Revision D.01)*, Gaussian Inc. Wallingford CT, 2009.
- 26 X. Y. Shen, Y. J. Wang, H. Zhang, A. Qin, J. Z. Sun and B. Z. Tang, *Chem. Commun.*, 2014, **50**, 8747.

the solution nor they lead to the recovery of fluorescence in the solid-state light.



Fluorescence

Solution		
Solid		
Color		

Table on contents graphic:

Tetraphenylethylene moieties conjugated with dipyrromethane core neither quench emission in